

# Experimental Constraints on Scharm-Stop Flavor Mixing and Implications in Top-quark FCNC Processes

Junjie Cao<sup>1</sup>, Gad Eilam<sup>1</sup>, Ken-ichi Hikasa<sup>2</sup>, Jin Min Yang<sup>3</sup>

<sup>1</sup> *Physics Department, Technion, 32000 Haifa, Israel*

<sup>2</sup> *Department of Physics, Tohoku University, Sendai 980-8578, Japan*

<sup>3</sup> *Institute of Theoretical Physics, Academia Sinica, Beijing 100080, China*

We examine experimental constraints on scharm-stop flavor mixing in the minimal supersymmetric standard model, which arise from the experimental bounds on squark and Higgs boson masses, the precision measurements of  $W$ -boson mass and the effective weak mixing angle, as well as the experimental data on  $B_s - \bar{B}_s$  mixing and  $b \rightarrow s\gamma$ . We find that the combined analysis can put rather stringent constraints on  $\tilde{c}_L - \tilde{t}_L$  and  $\tilde{c}_L - \tilde{t}_R$  mixings. As an illustration for the effects of such constraints, we examine various top-quark flavor-changing neutral-current processes induced by scharm-stop mixings at the LHC and find that their maximal rates are significantly lowered.

14.80.Ly, 11.30.Hv

**Introduction** It is well known that in the minimal supersymmetric standard model (MSSM), besides CKM matrix, flavor mixings in sfermion sector are another source of flavor violation [1]. Since such mixings arise from soft breaking terms, they relate flavor problem to SUSY breaking and their information may provide guidelines for SUSY model building. While such mixings can be directly measured through the flavor-changing decays of sfermions at future colliders [2], their information can also be obtained from various low energy processes [1,3]. So far the flavor mixings involving the first-generation squarks have been severely constrained by  $K^0 - \bar{K}^0$ ,  $D^0 - \bar{D}^0$  and  $B_d^0 - \bar{B}_d^0$  mixings [1], but the mixings between second- and third-generation squarks, especially the scharm-stop mixings, are less constrained. For example, although the electric dipole moment of mercury atom has been precisely measured, it only constrains the product of the  $\tilde{c}_L - \tilde{t}_L$  mixing with another undetermined free parameter [4]. Without definite information about the parameter, the constraint is ambiguous.

Scharm-stop mixings are well motivated in popular flavor-blind SUSY breaking models like supergravity models (SUGRA). In these models, the flavor-diagonality is usually assumed in sfermion mass matrices at the grand

unification scale and the Yukawa couplings induce flavor mixings when the sfermion mass matrices evolve down to the weak scale. Such radiatively induced off-diagonal squark-mass terms are proportional to the corresponding Yukawa couplings and thus the mixings between second- and third-generation squarks may be sizable [5].

Scharm-stop mixings can induce various top-quark flavor-changing neutral-current (FCNC) processes which will be tested at the CERN Large Hadron Collider (LHC). Given the importance of such mixings, we in this work examine current experimental constraints on them from the following considerations. Firstly, since the mixing terms appear as the non-diagonal elements of squark mass matrices, they can affect the squark mass spectrum, especially enlarge the mass splitting between squarks. So they should be constrained by the squark mass bounds from the direct experimental searches. At the same time, since the squark loops affect the precision electroweak quantities such as  $M_W$  and the effective weak mixing angle  $\sin^2\theta_{eff}$ , such mixings could be also constrained by the precision electroweak measurements. As will be shown later, to a good approximation, the supersymmetric corrections to the electroweak quantities are through the parameter  $\delta\rho$  and thus sensitive to the mass splitting of squarks. Secondly, the processes of  $b \rightarrow s$  transition like  $B_s - \bar{B}_s$  mixings and  $b \rightarrow s\gamma$  can provide rich information about the  $\tilde{s} - \tilde{b}$  mixings. Through the SU(2) relation between up-squark and down-squark mass matrices (see eq.(4)) and also through the electroweak quantities (since all squarks contribute to electroweak quantities via loops), the information can be reflected in up-squark sector and hence constrain the scharm-stop mixings. Thirdly, we note that the chiral flipping mixings of scharm-stop come from the trilinear  $H_2\tilde{Q}\tilde{U}$  interactions [1]. Such interactions can lower the lightest Higgs boson mass  $m_h$  via squark loops and thus should be subject to the current experimental bound on  $m_h$ .

We noticed that the constraints on scharm-stop mixings from  $m_h$  and  $\delta\rho$  have been discussed in [6]. But the

analyses of [6] focus on  $\tilde{c}_L - \tilde{t}_L$  mixing and did not consider  $\tilde{c}_L - \tilde{t}_R$ ,  $\tilde{c}_R - \tilde{t}_L$  and  $\tilde{c}_R - \tilde{t}_R$  mixings. Also, in [6] the authors ignored the  $SU(2)$  relation between the up- and down-squark mass matrices, and for the up-squark mass matrix, they left out the first generation and only considered the second and third generations. As will be discussed later, a complete consideration of three generations is necessary in calculating  $\delta\rho$ . Moreover, since the analyses of [6] focus on  $m_h$  and  $\delta\rho$  constraints, other constraints like  $B_s - \bar{B}_s$  mixing and  $b \rightarrow s\gamma$  are not included in [6].

In this work we will give a comprehensive analysis on the scharm-stop mixings. We will consider all possible mixings between scharms and stops, namely  $\tilde{c}_L - \tilde{t}_L$  and  $\tilde{c}_L - \tilde{t}_R$  mixings for left-handed scharm and  $\tilde{c}_R - \tilde{t}_L$  and  $\tilde{c}_R - \tilde{t}_R$  mixings for right-handed scharm. We will not only consider the constraints from  $m_h$  and  $\delta\rho$ , but also include the constraints from  $B_s - \bar{B}_s$  mixing and  $b \rightarrow s\gamma$ . As an illustration for the effects of such constraints, we will examine various top-quark FCNC processes induced by these scharm-stop mixings at the LHC.

**Calculations** Instead of presenting the detailed and lengthy analytic results, we just delineate the strategies of our calculations.

1. *Squark mass:* In the super-KM basis with states  $(\tilde{u}_L, \tilde{c}_L, \tilde{t}_L, \tilde{u}_R, \tilde{c}_R, \tilde{t}_R)$  for up-squarks and  $(\tilde{d}_L, \tilde{s}_L, \tilde{b}_L, \tilde{d}_R, \tilde{s}_R, \tilde{b}_R)$  for down-squarks, the  $6 \times 6$  squark mass matrix  $\mathcal{M}_{\tilde{q}}^2$  ( $\tilde{q} = \tilde{u}, \tilde{d}$ ) takes the form [1]

$$\mathcal{M}_{\tilde{q}}^2 = \begin{pmatrix} (M_{\tilde{q}}^2)_{LL} + C_{\tilde{q}}^{LL} & (M_{\tilde{q}}^2)_{LR} - C_{\tilde{q}}^{LR} \\ ((M_{\tilde{q}}^2)_{LR} - C_{\tilde{q}}^{LR})^\dagger & (M_{\tilde{q}}^2)_{RR} + C_{\tilde{q}}^{RR} \end{pmatrix}, \quad (1)$$

where  $C_{\tilde{q}}^{LL} = m_{\tilde{q}}^2 + \cos 2\beta M_Z^2 (T_3^q - Q_q s_W^2) \hat{1}$ ,  $C_{\tilde{q}}^{RR} = m_{\tilde{q}}^2 + \cos 2\beta M_Z^2 Q_q s_W^2 \hat{1}$  and  $C_{\tilde{q}}^{LR} = m_q \mu (\tan \beta)^{-2T_3^q}$  are  $3 \times 3$  diagonal matrices ( $\hat{1}$  stands for the unit matrix in flavor space and  $m_q$  is the diagonal quark mass matrix). Here,  $T_3^q = 1/2$  for up-squarks and  $T_3^q = -1/2$  for down-squarks, and  $\tan \beta = v_2/v_1$  is the ratio of the vacuum expectation values of the Higgs fields. In general, the soft mass parameters  $(M_{\tilde{q}}^2)_{LL}$ ,  $(M_{\tilde{q}}^2)_{LR}$  and  $(M_{\tilde{q}}^2)_{RR}$  are  $3 \times 3$  non-diagonal matrices. For up-squarks, if we only consider the flavor mixings between scharms and stops, then

$$\begin{aligned} (M_{\tilde{u}}^2)_{LL} &= \begin{pmatrix} M_{Q_1}^2 & 0 & 0 \\ 0 & M_{Q_2}^2 & \delta_{LL} M_{Q_2} M_{Q_3} \\ 0 & \delta_{LL} M_{Q_2} M_{Q_3} & M_{Q_3}^2 \end{pmatrix}, \\ (M_{\tilde{u}}^2)_{LR} &= \begin{pmatrix} 0 & 0 & 0 \\ 0 & 0 & \delta_{LR} M_{Q_2} M_{U_3} \\ 0 & \delta_{RL} M_{U_2} M_{Q_3} & m_t A_t \end{pmatrix}, \\ (M_{\tilde{u}}^2)_{RR} &= (M_{\tilde{u}}^2)_{LL} |_{M_{Q_i}^2 \rightarrow M_{D_i}^2, \delta_{LL} \rightarrow \delta_{RR}}. \end{aligned} \quad (2)$$

Similarly, for down-squarks we have

$$\begin{aligned} (M_{\tilde{d}}^2)_{LR} &= \begin{pmatrix} 0 & 0 & 0 \\ 0 & 0 & \delta_{LR}^d M_{Q_2} M_{D_3} \\ 0 & \delta_{RL}^d M_{D_2} M_{Q_3} & m_b A_b \end{pmatrix}, \\ (M_{\tilde{d}}^2)_{RR} &= (M_{\tilde{u}}^2)_{LL} |_{M_{Q_i}^2 \rightarrow M_{D_i}^2, \delta_{LL} \rightarrow \delta_{RR}^d}, \end{aligned} \quad (3)$$

and, due to  $SU_L(2)$  gauge invariance,  $(M_{\tilde{d}}^2)_{LL}$  is determined by [1]

$$(M_{\tilde{d}}^2)_{LL} = V_{CKM}^\dagger (M_{\tilde{u}}^2)_{LL} V_{CKM}. \quad (4)$$

Note that for the diagonal elements of left-right mixings in eqs.(2~3), we only kept the terms of third-family squarks since we adopted the popular assumption that they are proportional to the corresponding quark masses.

The squark mass eigenstates can be obtained by diagonalizing the mass matrix in eq.(1) with an unitary rotation  $U_{\tilde{q}}$ , which is performed numerically in our analysis. The interactions of a vector or scalar boson  $X$  with a pair of squark mass eigenstates are then obtained by

$$V(X \tilde{q}_\alpha^* \tilde{q}'_\beta) = U_{\tilde{q}}^{\dagger \alpha, i} U_{\tilde{q}'}^{j, \beta} V(X \tilde{q}_i^* \tilde{q}'_j), \quad (5)$$

where  $V(X \tilde{q}_i^* \tilde{q}'_j)$  denotes a generic vertex in the interaction basis and  $V(X \tilde{q}_\alpha^* \tilde{q}'_\beta)$  is the vertex in the mass-eigenstate basis. It is clear that both the squark masses and their interactions depend on the mixing parameters in the squark mass matrices.

Although we in eq.(2) listed all four possible mixings between scharms and stops, in the following we mainly focus on the mixings  $\delta_{LL}$  and  $\delta_{LR}$  for the left-handed scharm, and only give some brief discussions about the mixings  $\delta_{RL}$  and  $\delta_{RR}$  for the right-handed scharm. Our peculiar interest in  $\delta_{LL}$  and  $\delta_{LR}$  is based on the following two considerations. The first is that in the popular mSUGRA model, at the weak scale the flavor mixings for the left-handed scharm are proportional to bottom quark mass while those for the right-handed scharm are proportional to charm quark mass [5]. Therefore, in phenomenological studies of scharm-stop mixings, one usually assume the existence of  $\delta_{LL}$  and  $\delta_{LR}$ . The second is that  $\delta_{LL}$  and  $\delta_{LR}$  have richer phenomenology than  $\delta_{RL}$  and  $\delta_{RR}$ .  $\delta_{LL}$  and  $\delta_{LR}$  contribute sizably to all considered quantities, namely  $\delta\rho$ ,  $m_h$ ,  $B_s - \bar{B}_s$  mixing and  $b \rightarrow s\gamma$ , while  $\delta_{RL}$  and  $\delta_{RR}$  only affect  $\delta\rho$  and  $m_h$ .

2.  *$b \rightarrow s\gamma$ :* It has long been known that for  $b \rightarrow s\gamma$  the sizable SUSY contributions may come from three kinds of loops mediated respectively by the charged Higgs bosons, charginos and gluinos [7]. In our analysis we consider all these three kinds of loops plus those mediated by the neutralinos. We use the formula in [3], which includes all these SUSY loop effects in addition to the SM contribution. So, besides down-squark and up-squark mass parameters, our results also depend on charged Higgs boson mass, gaugino mass  $M_2$  and gluino mass  $m_{\tilde{g}}$ . As pointed out in numerous papers,  $b \rightarrow s\gamma$  is very sensitive

to  $\delta_{LR}^d$  and  $\delta_{RL}^d$ , and in some cases also sensitive to  $\delta_{LL}$  and  $\delta_{RR}$ .

3.  *$B_s - \bar{B}_s$  mixing:* In the MSSM the charged Higgs and chargino contributions to  $B_s - \bar{B}_s$  mixing are much suppressed compared with the gluino effects and the SM prediction [8]. So in our analysis we only include the gluino effects in addition to the SM contribution. We evaluate the gluino contributions by the full expressions, namely, without the mass-insertion approximation. Our Wilson coefficients are coincide with those in [9] and we use the formula in [8] to get the transition matrix element  $M_{12}$ . As pointed out in [8],  $B_s - \bar{B}_s$  mixing is very sensitive to the combination  $\delta_{LL}^d \delta_{RR}^d$  and  $\delta_{LR}^d \delta_{RL}^d$ , and with the current measurement of  $B_s - \bar{B}_s$  mixing [10], it can put rather severe constraints on  $\delta^d$ s.

4.  *$\delta M_W$  and  $\delta \sin^2 \theta_{eff}$ :* In the MSSM the corrections to  $M_W$  and  $\sin^2 \theta_{eff}$  are dominated by squark loops<sup>1</sup>. In our calculations we used the complete formula in [11] for the corrections. We checked that, to a good approximation (at the level of a few percent), they can be determined from the  $\delta\rho$  parameter [6]

$$\delta M_W \simeq \frac{M_W}{2} \frac{c_W^2}{c_W^2 - s_W^2} \delta\rho, \quad (6)$$

$$\delta \sin^2 \theta_{eff} \simeq -\frac{c_W^2 s_W^2}{c_W^2 - s_W^2} \delta\rho, \quad (7)$$

where

$$\delta\rho = \frac{\Sigma_Z(0)}{M_Z^2} - \frac{\Sigma_W(0)}{M_W^2}. \quad (8)$$

Although our results are not sensitive to the soft mass parameters of the first-generation squarks, we stress the necessity to consider all three generations of squarks in the calculations. The reason is the calculation of the squark loops in  $W$ -boson self-energy involves the couplings of  $W\tilde{u}_i\tilde{d}_j$ , which are given by  $U_{\tilde{u}}^\dagger V_{CKM} U_{\tilde{d}}$  with  $U_{\tilde{u}}$  and  $U_{\tilde{d}}$  defined in eq.(5). Only by considering all three generations of squarks can one get exact UV-convergent results and implement the SU(2) relation in eq.(4) at the same time. In [6] the authors only considered two generations of squarks (ignored the first generation) and by introducing an unphysical  $2 \times 2$  unitary matrix they kept their results free of UV-divergence. We checked numerically that such an approximation is not so good. For example, with the same parameters for the lowest curve of Fig.8 in [6], our result is  $\delta M_W = 11$  MeV for  $\delta_{LL} = 0.6$ , smaller than 40 MeV obtained in [6]. The main reason for

such sizable difference is due to the difference of  $W\tilde{u}_i\tilde{d}_j$  couplings. The matrices  $U_{\tilde{u}}$  and  $U_{\tilde{d}}$  of [6] are different from ours since they did not consider the SU(2) relation between up- and down-squark mass matrices, and the matrix  $V_{CKM}$  of [6] is also different from ours since we used the exact  $3 \times 3$  CKM matrix while they used an approximated  $2 \times 2$  unitary matrix. Due to the strong cancellation between different Feynman diagrams in the calculation of  $\delta\rho$ , the small difference of  $W\tilde{u}_i\tilde{d}_j$  couplings may lead to sizable difference in the final result.

5. *Higgs boson mass:* In the MSSM the loop-corrected lightest Higgs boson mass  $m_h$  is defined as the pole of the corrected propagator matrix, which can be obtained by solving the equation [12]

$$\begin{aligned} & \left[ p^2 - m_{h,tree}^2 + \hat{\Sigma}_{hh}(p^2) \right] \\ & \times \left[ p^2 - m_{H,tree}^2 + \hat{\Sigma}_{HH}(p^2) \right] - \left[ \hat{\Sigma}_{hH}(p^2) \right]^2 = 0, \end{aligned} \quad (9)$$

where  $m_{h,tree}$  and  $m_{H,tree}$  are the tree-level masses of  $h$  and  $H$ . To obtain the renormalized self-energies  $\hat{\Sigma}_i(p^2)$ , one needs to calculate Higgs boson self-energy and tad-pole diagrams and then organize the results by eq.(3.1) in [12]. Due to the large top-quark Yukawa couplings, the contribution from top and stop loops is far dominant among all SUSY contributions. In the presence of flavor mixings in the up-squark mass matrix, stops will mix with other squarks, and in this case, the dominant contribution comes from up-squark sector. In our calculation of  $m_h$ , we take into account this part of contribution as in [6]. For  $\delta_{LR,RL} = 0$ , we can reproduce the results in [6], but our results include  $\delta_{LR,RL} \neq 0$  case.

With the parametrization of the squark mass matrices in eqs.(2~4) and for small flavor mixing parameters of down-squarks, the quantities  $\delta M_W$ ,  $\delta \sin^2 \theta_{eff}$  and  $m_h$  are sensitive to the soft masses  $M_{Q_{2,3}}$  and  $M_{U_{2,3}}$ , the trilinear coupling  $A_t$  as well as  $\delta_{LR,RL}$ . And in some cases, they are also sensitive to  $\mu$ , the CP-odd Higgs boson mass  $m_A$  and  $\delta_{LL,RR}$ . Unlike  $B_s - \bar{B}_s$  mixing and  $b \rightarrow s\gamma$ , these quantities are not sensitive to gluino mass.

**Numerical results** To numerically illustrate the constraints on charm-stop mixing parameters  $\delta_{LL}$  and  $\delta_{LR}$ , we need to fix other involved parameters. Here, as an illustration, we consider the so-called  $m_h^{max}$  scenario, in which  $m_h$  can be maximized [13]. In this scenario, all the soft mass parameters are assumed to be degenerate

$$M_{SUSY} = M_{Q_i} = M_{U_i} = M_{D_i}, \quad (10)$$

and the trilinear couplings are also assumed to be degenerate  $A_{u_i} = A_{d_i}$  with  $(A_{u_i} - \mu \cot \beta)/M_{SUSY} = 2$ . Other SUSY parameters are fixed as  $\tan \beta = 10$ ,  $\mu = M_2 = m_A = m_{\tilde{g}} = 300$  GeV and  $\delta_{RL} = \delta_{RR} \delta_{LR}^d = \delta_{RL}^d =$

<sup>1</sup>Slepton contribution to  $\delta M_W$  and  $\delta \sin^2 \theta_{eff}$  is not important partially because slepton is SU(3) color singlet, and partially because, due to absence of large  $\tilde{l}_L - \tilde{l}_R$  mixing, the slepton SU(2) doublet  $(\tilde{\nu}, \tilde{l})$  are nearly degenerate, hence their contribution to  $\delta\rho$  tends to vanish [11].

$\delta_{RR}^d = 0$ . All the SM parameters involved in our calculations like  $M_Z$  are taken from the Particle Data Book [14].

We show in Fig.1 the constraints on the mixing parameters  $\delta_{LL}$  and  $\delta_{LR}$ . Here we used the LEP experimental bounds on squark mass [14] and Higgs boson mass [15]

$$m_{\tilde{u}} > 95.7 \text{ GeV}, \quad m_{\tilde{d}} > 89 \text{ GeV}, \quad m_h > 92.8 \text{ GeV}, \quad (11)$$

and required the MSSM loop contributions to  $M_W$  and  $\sin^2 \theta_{eff}$  not exceeding the present experimental uncertainties [16]

$$\Delta M_W < 34 \text{ MeV}, \quad \Delta \sin^2 \theta_{eff} < 15 \times 10^{-5}. \quad (12)$$

We also used the current measurement of  $b \rightarrow s\gamma$  at  $3\sigma$  level [17]

$$2.53 \times 10^{-4} < Br(b \rightarrow s\gamma) < 4.34 \times 10^{-4}, \quad (13)$$

and current favored region for  $B_s - \bar{B}_s$  mixing [18,10]

$$0.55 < |1 + R| < 1.37 \quad (14)$$

where  $R = M_{12}^{SUSY} / M_{12}^{SM}$ .

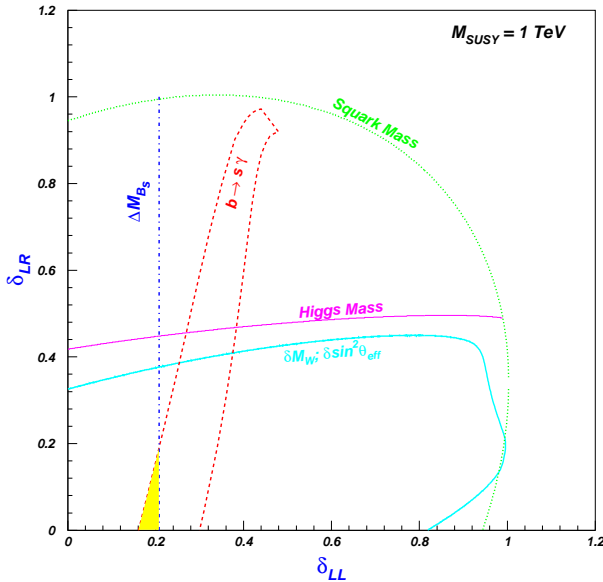


FIG. 1. The shaded area is allowed by all constraints. The dashed-line enclosed area is allowed by  $b \rightarrow s\gamma$ . For other individual constraints, the region under or left to each curve is the corresponding allowed region.

From Fig.1 we see that although the constraint from squark mass is rather weak, the combined constraints from  $b \rightarrow s\gamma$ ,  $B_s - \bar{B}_s$  mixing,  $\delta M_W$ ,  $\delta \sin^2 \theta_{eff}$  and  $m_h$  are quite strong and only a small area in  $\delta_{LL} - \delta_{LR}$  plane survives. We make following explanations about our results:

- (1) With our fixed parameters, the charged Higgs and chargino contributions enhance the SM prediction

of  $b \rightarrow s\gamma$  and thus a none-zero gluino contribution is needed to cancel the effects. Therefore, the  $b \rightarrow s\gamma$  allowed region is an enclosed one in Fig.1

- (2) In the case we considered,  $\delta M_W$  and  $\delta \sin^2 \theta_{eff}$  require a small  $\delta_{LR}$ . The reason is that the large splitting between  $\delta_{LR}$  and  $\delta_{LR}^d$  can spoil the custodial symmetry between squark doublet and hence enhance the value of  $\delta\rho$ . In our calculations we fixed  $\delta_{LR}^d = 0$ , but we checked that the maximal allowed value of  $\delta_{LR}$  is not sensitive to  $\delta_{LR}^d$  if  $\delta_{LR}^d < 0.4$ . For example, when  $\delta_{LR}^d$  varies from 0 to 0.4, the maximal value of  $\delta_{LR}$  only increases by 0.05. Note that compared with  $\delta_{LR}$ ,  $\delta M_W$  and  $\delta \sin^2 \theta_{eff}$  are less sensitive to  $\delta_{LL}$ .
- (3) The Higgs mass  $m_h$  requires a small  $\delta_{LR}$  because  $\delta_{LR}$  comes from  $H_2 \tilde{c}_L^* \tilde{t}_R$  interaction which can lower the value of  $m_h$  via squark loops.
- (4) With our fixed parameters,  $B_s - \bar{B}_s$  mixing and  $b \rightarrow s\gamma$  give the stronger constraint on  $\delta_{LR}$  than  $\delta\rho$  and  $m_h$ , but in other cases,  $\delta\rho$  or  $m_h$  may give the strongest constraints. For example, in  $m_h^{max}$  scenario with  $M_{SUSY} = 2 \text{ TeV}$ , the Higgs mass constraint becomes the strongest.

Note that in the above we only show the constraints on  $\delta_{LL}$  and  $\delta_{LR}$ . Now we take a look at  $\delta_{RL}$  and  $\delta_{RR}$ . Since  $B_s - \bar{B}_s$  mixing and  $b \rightarrow s\gamma$  are not sensitive to  $\delta_{RL}$  and  $\delta_{RR}$ , the constraints are then only from  $\delta\rho$  and  $m_h$ . We found that  $\delta\rho$  requires a small  $\delta_{RL}$  (the constraint is similar to  $\delta_{LR}$ ), but is insensitive to  $\delta_{RR}$ . Just like  $\delta_{LR}$ , a small  $\delta_{RL}$  is also required by the Higgs mass  $m_h$ . Therefore,  $\delta_{RL}$  is constrained by  $\delta\rho$  and  $m_h$  just like  $\delta_{LR}$ ; while  $\delta_{RR}$  is very weakly constrained.

**Implication in top-quark FCNC process:** With the constraints discussed above, we examined various top-quark FCNC decay and production processes at the LHC, some of which were intensively studied in the literature [19–21]. We just considered the dominant SUSY-QCD contributions to these processes. The detailed calculations, the results and the discussions of observability are quite lengthy and will be presented in another paper. Here, as an illustration of the effects of the constraints discussed in this paper, we only show in Table 1 the maximal results predicted by the MSSM. These maximal results are obtained by scanning the relevant SUSY parameters in the ranges

$$\begin{aligned} 2 < \tan \beta < 60, \quad 0 < M_{Q_i, U_i, D_i} < 1 \text{ TeV}, \\ 94 \text{ GeV} < m_A < 1 \text{ TeV}, \quad 195 \text{ GeV} < m_{\tilde{g}} < 1 \text{ TeV}, \\ 0 < \delta_{LL, LR} < 1, \quad -1 \text{ TeV} < \mu, M_2 < 1 \text{ TeV}, \\ 0 < \delta_{LR}^b < 0.1, \quad -2 \text{ TeV} < A_{t,b} < 2 \text{ TeV}. \end{aligned} \quad (15)$$

We show in Table I two kinds of predictions: one is by requiring the squark, chargino and neutralino masses satisfy their current lower bounds; the other is by imposing

all constraints considered in this paper. We consider two cases: (I) only  $\delta_{LL} \neq 0$  and (II) only  $\delta_{LR} \neq 0$ . From Table I we see that the combined constraints can significantly decrease the MSSM predictions of top-quark FCNC processes at the LHC.

Note that in Table I we only illustrate the cases of  $\delta_{LL} \neq 0$  and  $\delta_{LR} \neq 0$ . For  $\delta_{RL} \neq 0$ , we found that the maximum rate of  $t \rightarrow cg$  is  $1.3 \times 10^{-4}$  with only the squark mass constraints and changed to  $6 \times 10^{-5}$  with all constraints. For  $\delta_{RR} \neq 0$ , the maximum rate of  $t \rightarrow cg$  is  $5.0 \times 10^{-5}$  with only the squark mass constraints and changed to  $4.85 \times 10^{-5}$  with all constraints. This can be easily understood since, as discussed earlier,  $\delta_{RR}$  is very weakly constrained and  $\delta_{RL}$  is constrained by  $\delta\rho$  and  $m_h$ .

Table 1: Maximal predictions for top-quark FCNC processes induced by stop-scharm mixings via gluino-squark loops in the MSSM. For the productions we show the hadronic cross sections at the LHC and include the corresponding charge-conjugate channels. For the decays we show the branching ratios.

	$\delta_{LL} \neq 0$		$\delta_{LR} \neq 0$	
	constraints masses	constraints all	constraints masses	constraints all
$cg \rightarrow t$	1450 fb	225 fb	3850 fb	950 fb
$gg \rightarrow t\bar{c}$	1400 fb	240 fb	2650 fb	700 fb
$cg \rightarrow t\bar{g}$	800 fb	85 fb	1750 fb	520 fb
$cg \rightarrow t\bar{\gamma}$	4 fb	0.4 fb	8 fb	1.8 fb
$cg \rightarrow t\bar{Z}$	11 fb	1.5 fb	17 fb	5.7 fb
$cg \rightarrow t\bar{h}$	550 fb	18 fb	12000 fb	24 fb
$t \rightarrow ch$	$1.2 \times 10^{-3}$	$2.0 \times 10^{-5}$	$2.5 \times 10^{-2}$	$6.0 \times 10^{-5}$
$t \rightarrow cg$	$5.0 \times 10^{-5}$	$5.0 \times 10^{-6}$	$1.3 \times 10^{-4}$	$3.2 \times 10^{-5}$
$t \rightarrow cZ$	$5.0 \times 10^{-6}$	$5.7 \times 10^{-7}$	$1.2 \times 10^{-5}$	$1.8 \times 10^{-6}$
$t \rightarrow c\gamma$	$9.0 \times 10^{-7}$	$1.5 \times 10^{-7}$	$1.3 \times 10^{-6}$	$5.2 \times 10^{-7}$

**Conclusion:** We examined current experimental constraints on scharm-stop flavor mixing in the MSSM, which arise from the experimental bounds on squark and Higgs boson masses, the precision measurements of the  $\delta\rho$  parameter, as well as the experimental data on  $B_s - \bar{B}_s$  mixing and  $b \rightarrow s\gamma$ . We found that the combined analysis of these constraints can severely constrain the  $\tilde{c}_L - \tilde{t}_L$  and  $\tilde{c}_L - \tilde{t}_R$  mixings; while the  $\tilde{c}_R - \tilde{t}_L$  mixing is constrained only by  $\delta\rho$  and Higgs mass, and the  $\tilde{c}_R - \tilde{t}_R$  mixing can almost elude any constraints. Such constraints can significantly alter the predictions of the top-quark FCNC processes induced by scharm-stop mixings at the LHC and thus should be taken into account in the study of observability of these top-quark FCNC processes.

**Acknowledgement:** This work is supported in part by the Israel Science Foundation, the Fund for the Promotion of Research at Technion, the Grant-in-Aid for Scientific Research (No. 14046201) from the Japan Ministry of Education, Culture, Sports, Science and Technology

and by the National Natural Science Foundation of China under Grant No. 10475107, 10505007 and 10375017.

- 
- [1] See, *e. g.*, S. Dimopoulos, D. Sutter, Nucl. Phys. **B452**, 496 (1996); F. Gabbiani, *et al.*, Nucl. Phys. **B477**, 321 (1996); M. Misiak, S. Pokorski, J. Rosiek, hep-ph/9703442.
  - [2] J. J. Cao, *et al.*, Phys. Rev. D **59**, 095001(1999); T. Han, *et al.*, Phys. Rev. D **70**, 055001 (2004).
  - [3] T. Besmer, C. Greub, T. Hurth, Nucl. Phys. **B609**, 359 (2001); F. Borzumati, *et al.*, Phys. Rev. D **62**, 075005(2000).
  - [4] M. Endo, M. Kakizaki, M. Yamaguchi, Phys. Lett. B **583**, 186(2004).
  - [5] K. Hikasa and M. Kobayashi, Phys. Rev. D **36**, 724 (1987); M. J. Duncan, Nucl. Phys. **B221**, 285 (1983).
  - [6] S. Heinemeyer, *et al.*, Eur. Phys. J. C **37**, 481 (2004).
  - [7] R. Barbieri and G. F. Giudice, Phys. Lett. B **309**, 86 (1993).
  - [8] P. Ball, S. Khalil and E. Kou, Phys. Rev. D **69**, 115011 (2004); M. Ciuchini, L. Silvestrini, hep-ph/0603114.
  - [9] J. M. Gérard, *et al.*, Phys. Lett. B **140**, 349, (1984); R. Harnik, *et al.*, Phys. Rev. D **69**, 094024 (2004).
  - [10] D0 Collaboration, hep-ex/0603029; CDF Collaboration, hep-ex/0606027.
  - [11] See, *e.g.*, P. Chankowski, *et al.*, Nucl. Phys. **B417**, 101 (1994); D. Garcia and J. Solà, Mod. Phys. Lett. **A 9**, 211 (1994).
  - [12] A. Dabelstein, Z. Phys. C **67**, 495 (1995).
  - [13] M. Carena, *et al.*, Eur. Phys. J. C **26**, 601 (2003).
  - [14] Particle Data Group, Phys. Lett. B **592**, 1 (2004).
  - [15] See, *e.g.*, A. Sopczak, hep-ph/0602136.
  - [16] The LEP Collaborations, hep-ex/0509008.
  - [17] HFAG Group, <http://www.slac.stanford.edu/xorg/hfag>.
  - [18] M. Endo and S. Mishima, hep-ph/0603251.
  - [19] For  $t \rightarrow cV$  in the MSSM, see, *e. g.*, C. S. Li, R. J. Oakes, J. M. Yang, Phys. Rev. D **49**, 293 (1994); G. Couture, C. Hamzaoui, H. Konig, Phys. Rev. D **52**, 1713 (1995); J. L. Lopez, D. V. Nanopoulos, R. Rangarajan, Phys. Rev. D **56**, 3100 (1997); G. M. de Divitiis, R. Petronzio, L. Silvestrini, Nucl. Phys. **B504**, 45 (1997); J. M. Yang, B.-L. Young, X. Zhang, Phys. Rev. D **58**, 055001 (1998).
  - [20] For  $t \rightarrow ch$  in the MSSM, see, *e. g.*, J. M. Yang, C. S. Li, Phys. Rev. D **49**, 3412 (1994); J. Guasch, J. Sòla, Nucl. Phys. **B562**, 3 (1999); G. Eilam, *et al.*, Phys. Lett. B **510**, 227 (2001); J. L. Diaz-Cruz, H.-J. He, C.-P. Yuan, Phys. Lett. B **530**, 179 (2002).
  - [21] J. Cao, Z. Xiong and J. M. Yang, Nucl. Phys. **B651**, 87 (2003); Phys. Rev. D **67**, 071701 (2003); J. J. Liu, *et al.*, Nucl. Phys. **B705**, 3 (2005); J. M. Yang, Annals Phys. **316**, 529 (2005); J. Guasch, *et al.*, hep-ph/0601218; G. Eilam, M. Frank, I. Turan, hep-ph/0601253.